



# Effect of RF Power on Structural, Magnetic, and Optical Properties of CoFe<sub>2</sub>O<sub>4</sub> Thin Films

Kancharla Ravi Babu<sup>1</sup> · R. Singh<sup>1</sup>

Received: 19 March 2018 / Accepted: 30 March 2018 / Published online: 12 April 2018  
© Springer Science+Business Media, LLC, part of Springer Nature 2018

## Abstract

The thin films of CoFe<sub>2</sub>O<sub>4</sub> were deposited on glass substrates by radio-frequency (RF) sputtering. The effect of RF power variation from 60–120 W on the structure, magnetic, and optical properties of the as-deposited films and films annealed at 500 °C was studied. The magnetic parameters of the film, i.e., in-plane coercivity ( $H_c$ ), saturation magnetization ( $M_s$ ), and remanence ( $M_r$ ) increase as RF power is increased from 60 to 80 W followed by a decreasing trend with further increase in RF power to 120 W. Annealing of the film significantly improves the magnetic properties. The largest grain size and the best crystallinity of the film are obtained for the film deposited at 80 W of RF power. The thin films exhibited 70–80% optical transmittance. Optical band gap ( $E_g$ ) depends on the RF power and grain size, and it varies between 2.08 and 2.16 eV for the as-deposited films and between 2.16 and 2.30 eV for the annealed films. The study shows that RF power used for depositing the film has strong effect on the microstructure and properties of the film.

**Keywords** Cobalt ferrite · Thin films · RF magnetron sputtering · RF power · Magnetization · Optical band gap

## 1 Introduction

Cobalt-ferrite CoFe<sub>2</sub>O<sub>4</sub> (CFO) thin films have been investigated in recent years as one of the candidates for high-density magnetic recording and magneto-optical recording media because of their unique physical properties such as high Curie temperature, large magnetic anisotropy, moderate magnetization, and excellent chemical stability [1, 2]. The CFO has been used to fabricate heterostructures for spin filtering [3], resistive switching [4], and magneto-electric coupling between ferromagnetic and ferroelectric thin film layers [5]. The magnetic and optical studies on ferrites are reported in the literature [6, 7]. The band gap of 2.55 eV for CoFe<sub>2</sub>O<sub>4</sub> ferrite films deposited on (001)-oriented LaAlO<sub>3</sub> is reported [8]. Whereas, band gap of Zinc ferrite is reported to be around 2.2 eV [9]. Radio-frequency (RF) sputtering for depositing thin films is a useful technique as the properties of the films can be

controlled by changing the sputtering conditions such as substrate temperature, deposition time, pressure, and RF power. We have used this technique to synthesize Co-ferrite films at various RF powers. In this paper, we present the magnetization and optical data on thin films of Co-ferrite prepared at RF power of 60–120 W. Detailed systematic studies were undertaken on the as-deposited and annealed films of cobalt ferrite. These studies are helpful in tuning the properties of the ferrite films.

## 2 Experimental

Cobalt-ferrite thin films were deposited on glass substrates by RF magnetron sputtering technique, using stoichiometric ceramic CoFe<sub>2</sub>O<sub>4</sub> target. Prior to each deposition the vacuum chamber was pumped down to a base pressure of  $4 \times 10^{-5}$  Torr. The sputtering was done in Ar atmosphere with a target-to-substrate distance of 6 cm. The films were deposited on unheated substrates using RF power of 60, 80, 100, and 120 W, in argon gas environment at pressure of 10 mTorr for a deposition time of 1 h. The as-grown films were annealed in air at 500 °C for 3 h. Samples were identified with the RF power magnitudes used as CFF-60, CFF-80, CFF-100, and CFF-120. The details of sputtering system and film preparation are described in our earlier report [9].

✉ R. Singh  
rssp@uohyd.ernet.in; rsinghsp@gmail.com

<sup>1</sup> School of Physics, University of Hyderabad,  
Hyderabad 500046, India

The structure of the films was characterized by grazing incidence X-ray diffractometer (Bruker D8 discover) with Cu-K $\alpha$  source operating at 40 kV and 30 mA, field emission scanning electron microscopy, and transmission electron microscopy. Film thickness was measured using surface stylus profilometer (AMBIOS Tech Model XP-1). Magnetic properties of the films were measured by using LakeShore-7400 vibrating sample magnetometer and physical property measurement system (Quantum Design). The optical transmission spectra of the films were measured in the wavelength range of 200–2500 nm by using JASCO V570 spectrophotometer.

### 3 Results and Discussion

#### 3.1 Film Thickness

Thickness of the as-deposited films is estimated by using profilometer. The thickness of the film increases as the RF power increases. This is due to the increase in deposition rate with the increase in RF power [10]. A slight decrease in thickness of film was observed after annealing. This may be due to increase in packing density of the films on annealing. Film thickness for various films annealed at 500 °C for 3 h is shown in Fig. 8 and Table 3.

#### 3.2 Structural Analysis

The XRD patterns of the CoFe<sub>2</sub>O<sub>4</sub> target and the grazing incident angle X-ray diffraction patterns measured on the as-sputtered films as well as on the annealed films are shown in Fig. 1.

The X-ray peaks of the target and the films are in accordance with those of a typical crystalline Co ferrite, with spinel structure without a preferred orientation. The as-deposited films CFF-60 and CFF-80 are amorphous, while those deposited at higher RF power (100 and 120 W) show a certain degree of crystallinity. After annealing at 500 °C for 3 h, the major peaks corresponding to cobalt-ferrite emerge, indicating the improvement in crystallization. The XRD line width and crystallite size are connected through the Debye-Scherrer equation [11] given by  $D = 0.9\lambda / (\beta \cos \theta)$  where,  $D$  is crystallite size in amperes,  $\lambda$  is the wavelength of X-rays,  $\beta$  is the full width of the diffraction line at half the maximum intensity and  $\theta$  is the diffraction angle. The size of crystallites was calculated using the full width at half maximum (FWHM) of the (3 1 1) peak and the values are presented in Table 1. Nanocrystalline nature of Co-ferrite thin films is evident from the data. The calculated lattice parameter of Co-ferrite target is 8.346 Å and that of the films varies between 8.39 and 8.48 Å.

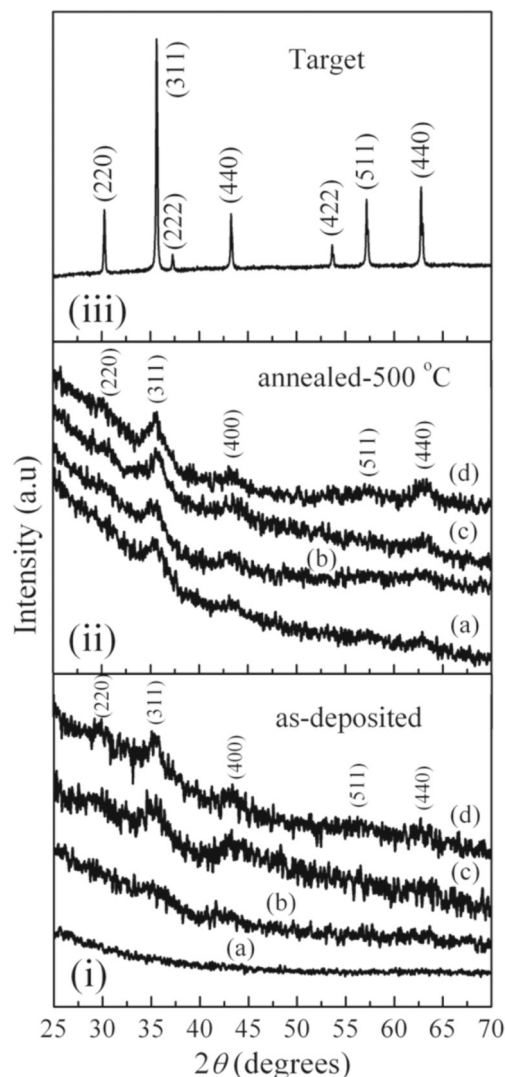


**Fig. 1** The XRD patterns of the CoFe<sub>2</sub>O<sub>4</sub> thin films grown at **a** 60, **b** 80, **c** 100, and **d** 120 W RF powers, for as-deposited (i), annealed at 500 °C (ii), and target (iii)

#### 3.3 Surface Morphology

Field emission scanning electron microscopy micrographs of the cobalt-ferrite films are shown in Figs. 2 (for as-deposited) and 3 (annealed). The grain-size distribution was determined from the histogram obtained by measuring the size of around 100–200 individual grains using image J software. For the as-deposited films, the average grain size is 44, 38, 47, and 42 nm for CFF-60, CFF-80, CFF-100, and CFF-120, respectively. For the annealed films, the histogram of sample CFF-60 shows that the maximum size distribution is in the range of 15–20 nm, for CFF-80, 15–25 nm, and for CFF-100 and CFF-120, it is in the range of 20–25 nm. Average grain size estimated by FESEM increases from 16 to 28 nm as RF power increases from 60 to 80 W and then

**Table 1** FESEM, TEM, and structural properties of annealed CoFe<sub>2</sub>O<sub>4</sub> thin films

Sample	Lattice constant 'a' (±0.01 Å)	Crystallite size (±2 nm) XRD	Grain size (±2 nm) as-deposited films	Grain size (±2 nm) annealed films	Particle size (±2 nm)
			FESEM	FESEM	TEM
CFF-60	8.43	11	44	18	11
CFF-80	8.48	19	38	28	19
CFF-100	8.34	10	47	22	11
CFF-120	8.39	13	42	21	9
Target	8.35	51	–	–	–

it decreases to 22 and 21 nm with a further increase in RF power of 100 and 120 W, respectively. The average values of grain size are listed in Table 1. Both sample CFF-80

(Fig. 3b) and sample CFF-120 (Fig. 3d) have polycrystalline structure. The largest crystal grain and the best crystallinity were obtained for film deposited at RF power of 80 W.

**Fig. 2** FESEM images of the CoFe<sub>2</sub>O<sub>4</sub> thin films grown at **a** 60, **b** 8, **c** 100, and **d** 120 W RF powers and cluster-size distribution

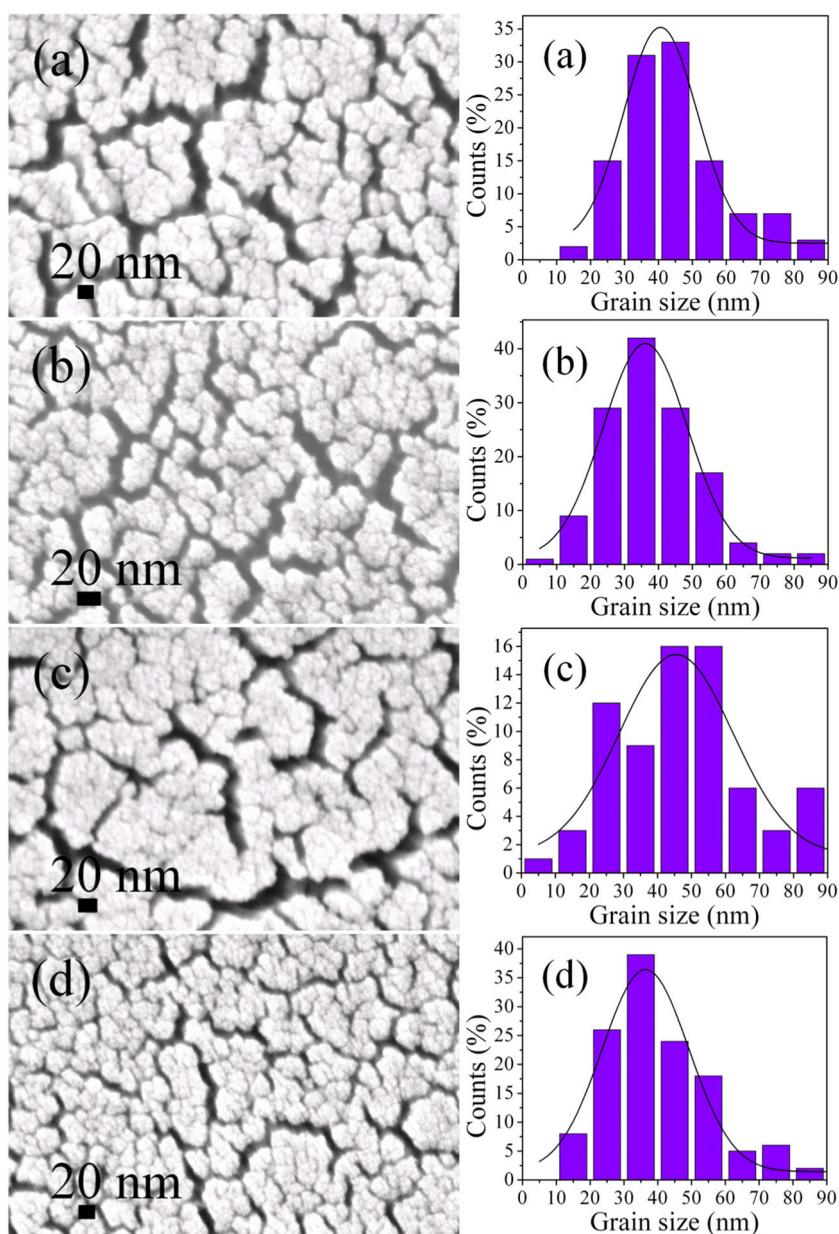
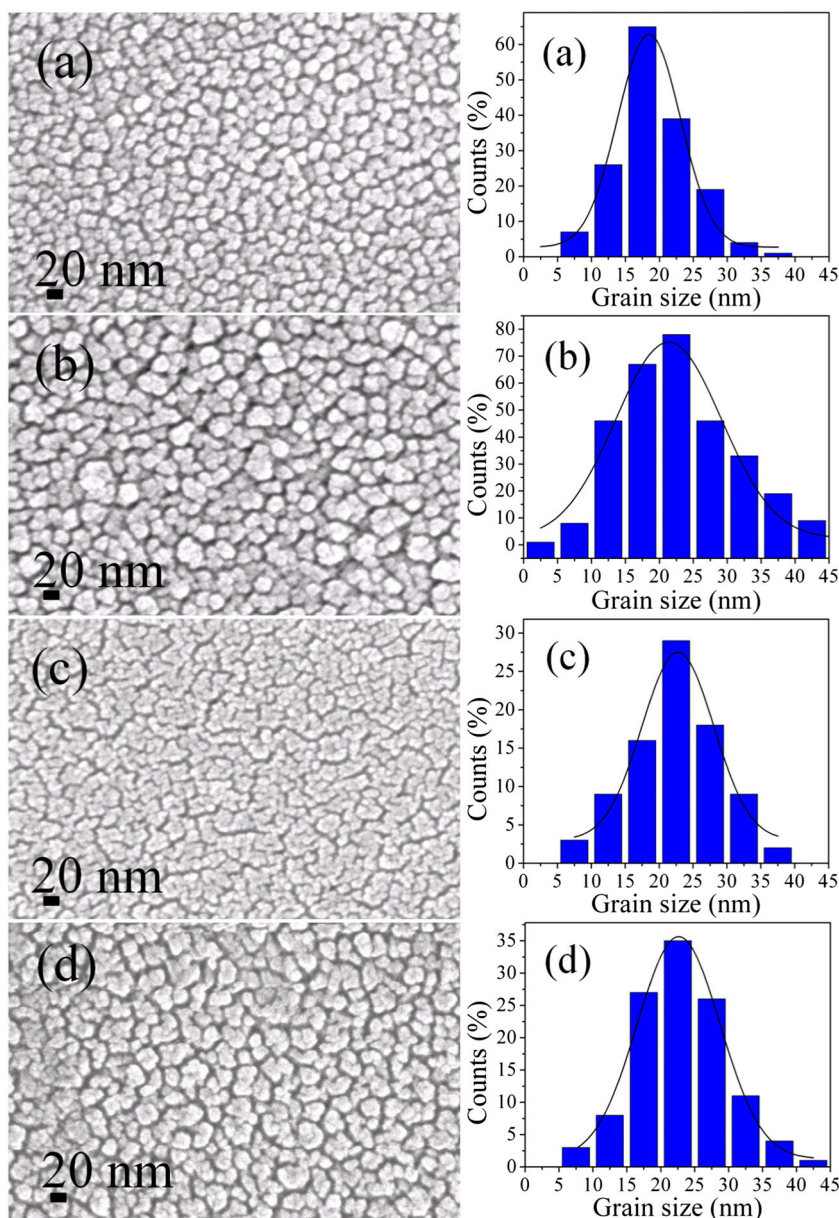




**Fig. 3** FESEM images of the annealed  $\text{CoFe}_2\text{O}_4$  thin films grown at **a** 60, **b** 8, **c** 100, and **d** 120 W RF powers and grain-size distribution



The surface morphology of the present film is very different from that reported by other group [12].

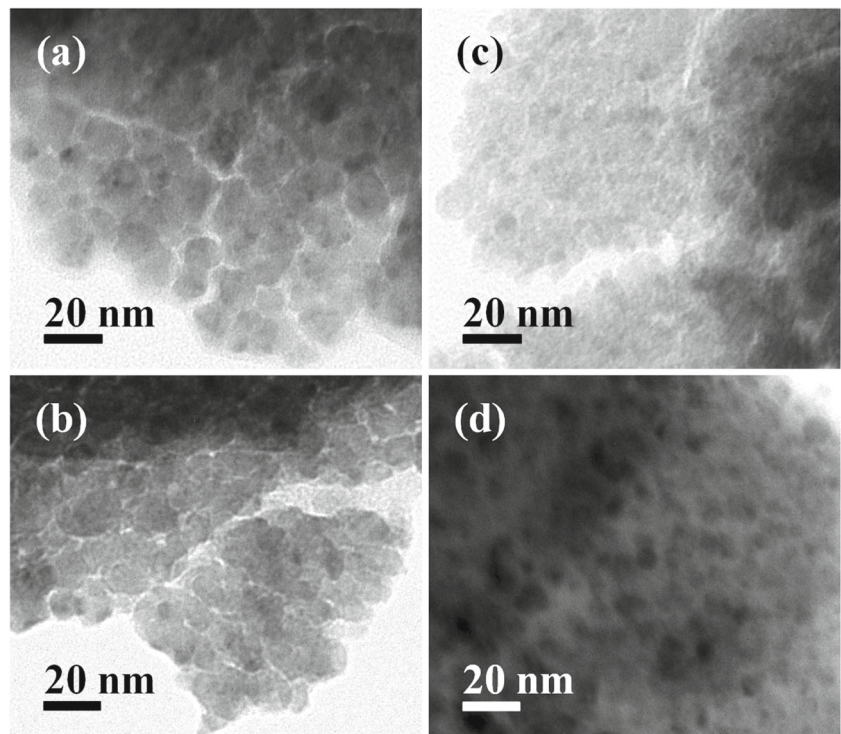
### 3.4 Transmission Electron Microscopy

Transmission electron microscopy (TEM) and high resolution microscopy have been used to confirm the nanocrystalline nature of the films. Figure 4 shows the TEM images of the annealed films. It can be seen that the particles are more or less spherical with an average size of 11, 19, 11, and 9 nm for CFF-60, CFF-80, CFF-100, and CFF-120, respectively (Table 1) These values are in agreement with the particle size estimated from xrd data using Scherrer formula.

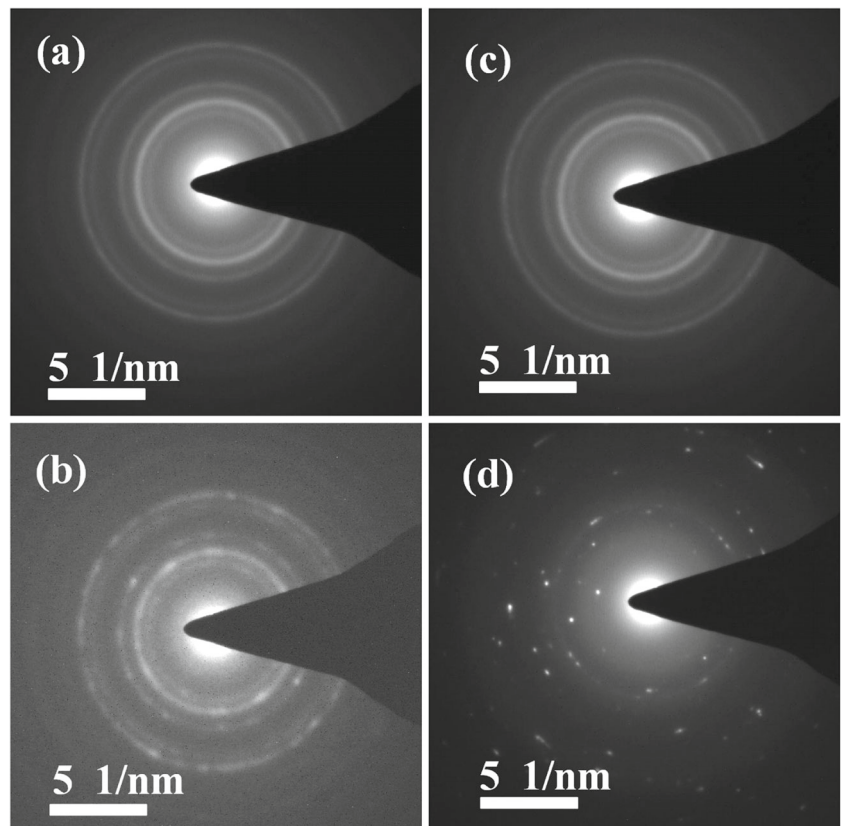
The selected area diffraction (SAD) patterns are shown in Fig. 5. The diameter of the diffraction ring in the SAD pattern is proportional to  $\sqrt{h^2 + k^2 + l^2}$  where (hkl) are the Miller indices of the planes corresponding to the ring. Counting the rings from the center 1st, 2nd, 3rd, 4th, and 5th rings correspond to (2 2 0), (3 1 1), (4 0 0), (5 1 1) and (4 4 0) planes, respectively.

The high-resolution TEM image of the annealed films in Fig. 6 show the lattice fringes of the nanocrystallites. The nanocrystal formation on annealing can be seen in Fig. 6b for thin film deposited at 80 W of RF power. These micrographs show details of the interplanar distance corresponding to different planes in spinel structure.

**Fig. 4** Microstructure of annealed  $\text{CoFe}_2\text{O}_4$  films by TEM grown at various RF powers: **a** 60, **b** 80, **c** 100, and **d** 120 W

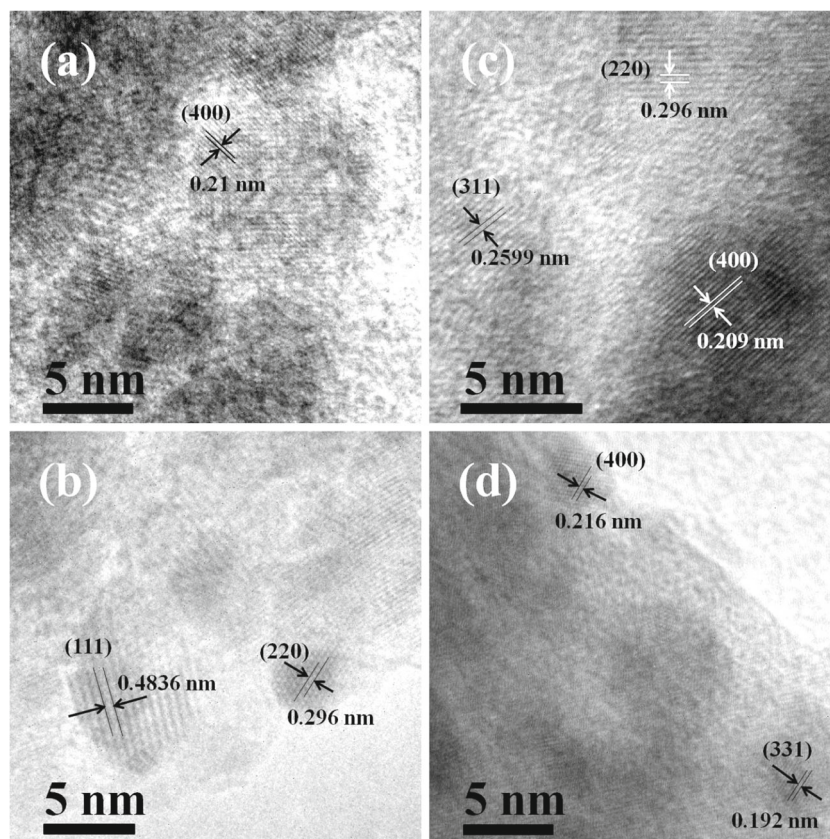


**Fig. 5** Selected area diffractions of annealed  $\text{CoFe}_2\text{O}_4$  films grown at various RF powers: **a** 60, **b** 80, **c** 100, and **d** 120 W





**Fig. 6** HRTEM micrographs of annealed  $\text{CoFe}_2\text{O}_4$  films grown at various RF powers: **a** 60, **b** 80, **c** 100, and **d** 120 W



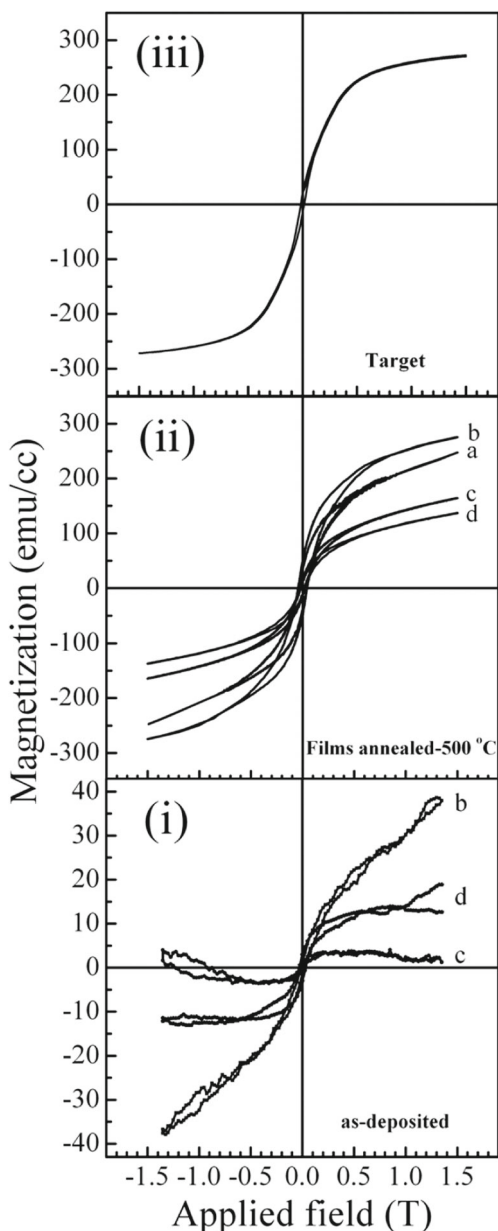
### 3.5 Magnetic and Optical Properties

Figure 7 shows the magnetization hysteresis loops of  $\text{CoFe}_2\text{O}_4$  target, as-deposited, and annealed thin films measured at room temperature. The loops were obtained with the magnetic field applied parallel to the plane of the film and corrected by subtracting the diamagnetic contribution from the substrate. Since the magnetization does not saturate up to a field of 1.5 T, so magnetization at the highest field value are compared for different films. The magnetization at 1.5 T ( $M_s$ ), remanent magnetization ( $M_R$ ), and coercivity ( $H_c$ ) of the films are tabulated in Table 2.

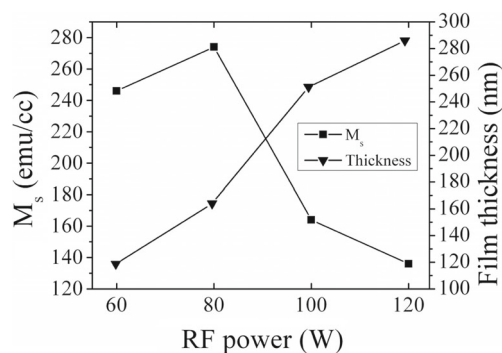
The as-deposited films are amorphous and have a small magnetization compared with that of the target. After annealing, the  $H_c$  and  $M_s$  values of the film increase significantly depending on film thickness. The target has  $H_c$  of 162 G and  $M_s$  of  $272 \text{ emu/cm}^3$ . The in-plane coercivities of the annealed film increase as the RF power increased from 60 to 80 W and then decreases with further increase in RF power up to 120 W. It is related to the increase in grain size up to 80 W followed by a decrease in grain size as RF power is increased to 120 W (Fig. 4).

Figure 8 shows the dependence of  $M_s$  at 1.5 T on RF power for the annealed films. The decrease in  $M_s$  of the annealed films can be explained in two ways. It can be due to the change in microstructure of the film as RF power

increases. The film deposited at 60 W is porous (Fig. 4), having an  $M_s$  value of  $246 \text{ emu/cm}^3$ . For the film grown at 80 W, the porosity decreases due to the fusion of grains forming bigger dense grains leading to an increase in  $M_s$  value to  $274 \text{ emu/cm}^3$  which is close to the bulk value. As the RF power is increased to 100 W, grains are loosely connected leading to a decrease in  $M_s$  to  $164 \text{ emu/cm}^3$ . The film deposited at an RF power of 120 W exhibits appearances of very large grain boundaries and hence the  $M_s$  value is further reduced to  $136 \text{ emu/cm}^3$ . The variation in  $M_s$  can be due to changes in cation distribution among the A and B sites due to heat treatment. The increase in  $M_s$  value of the film grown at 80 W (CFF-80) could be due to the disorder in the distribution of  $\text{Fe}^{3+}$  and  $\text{Co}^{2+}$  among A and B sites compared with a perfectly ordered inverse spinel structure. In the fully inverted structure, the  $\text{Fe}^{3+}$  moments are completely compensated and the net moment arises only from  $\text{Co}^{2+}$  ions. The occupation of  $\text{Co}^{2+}$  ions to octahedral sites might be less than the full. The octahedral holes which are not occupied by the  $\text{Co}^{2+}$  ions might be filled with  $\text{Fe}^{3+}$  ions which lead to the increase in  $M_s$  of the film CFF-80. The decrease in  $M_s$  of CFF-100 and CFF-120 could be related to the increase in cation ordering among A and B sites. The 164-nm (CFF-80) cobalt-ferrite film has a  $H_c$  of 442 Oe and  $M_s$  of  $274 \text{ emu/cm}^3$ , at room temperature (see Fig. 7; Table 2). Wang et al. [13] reported a  $H_c$  of 3.2 kOe



**Fig. 7** The magnetization hysteresis loops of CoFe<sub>2</sub>O<sub>4</sub> thin films grown at **a** 60, **b** 80, **c** 100, and **d** 120 W RF powers for as-deposited (i), annealed at 500 °C (ii), and CoFe<sub>2</sub>O<sub>4</sub> target (iii)



**Fig. 8** Dependence of magnetization ( $M_s$ ) at 1.5 T and film thickness of annealed CoFe<sub>2</sub>O<sub>4</sub> thin films deposited at various RF powers

and  $M_s$  of 291 emu/cm<sup>3</sup> for Co-ferrite films annealed at 900 °C and  $M_s$  value of 48 emu/cm<sup>3</sup> and  $H_c$  value of 50 Oe for 100-nm-thick Co-ferrite film annealed at 500 °C for 2 h. The present study shows that the  $H_c$  and  $M_s$  values strongly depend on thickness of the film when annealed at 500 °C for 2 h.

**Optical Properties** The optical transmittance spectra in the wavelength range of 200–2500 nm for CoFe<sub>2</sub>O<sub>4</sub> thin films grown at various RF powers for the as-deposited CoFe<sub>2</sub>O<sub>4</sub> thin films and annealed films are shown in Fig. 9. The fringes in the transmission spectra result from the interference of the incident light at the air-film, film-substrate, and substrate-air interfaces. Each spectrum can be roughly divided into three regions: (i) a zone of strong absorption in the near-UV region from 400 to 300 nm, transmittance decreases abruptly; (ii) a region of moderate absorption in the visible region from 400 to 750 nm, where the transmittance decreases drastically owing to the effect of the absorption coefficient; (iii) a transparent one with the interference pattern in the near-IR region between 760 and 2500 nm. The as-deposited films exhibit over 50% transmittance in the visible region and 84% in NIR region. The absorption edge of the as-deposited films is between 600 and 700 nm. The absorption edge shifts toward lower wavelength for the annealed films without any significant change in transmittance. In the medium absorption region ( $\lambda < 700$  nm), the transmittance spectra of the annealed

**Table 2** Magnetic and optical parameters of CoFe<sub>2</sub>O<sub>4</sub> thin films deposited at various RF powers

Sample	As-deposited films			Annealed films		
	$M_r$ (emu/cm <sup>3</sup> )	$M_s$ (emu/cm <sup>3</sup> )	$H_c$ (G)	$M_r$ (emu/cm <sup>3</sup> )	$M_s$ (emu/cm <sup>3</sup> )	$H_c$ (Oe)
CFF-60	–	–	–	36	246	402
CFF-80	1.5	38	181	50	274	442
CFF-100	0.3	2	75	15	164	220
CFF-120	2.4	14	313	12	136	154
Target	18	272	162			

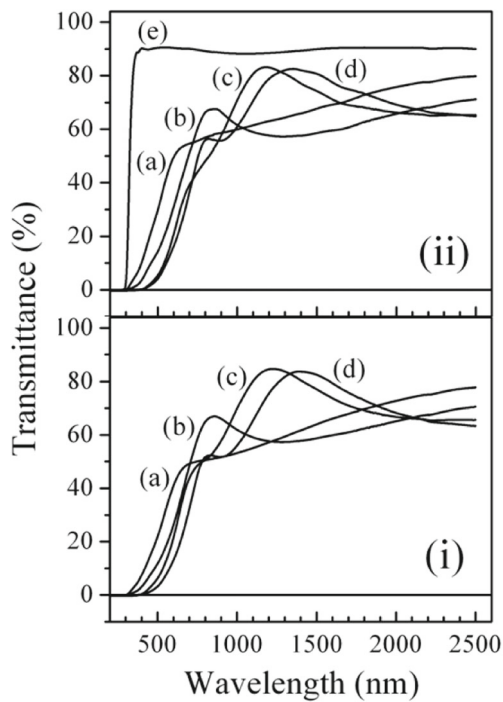


**Fig. 9** Optical transmittance spectra measured at RT of as-deposited (i), annealed (ii), CoFe<sub>2</sub>O<sub>4</sub> thin films grown at **a** 60, **b** 80, **c** 100, and **d** 120 W RF powers and **e** empty glass substrate

films are slightly shifted to shorter-wavelength (blue-shift) as compared with the as-deposited films. The absorption coefficient  $\alpha$  was determined from the optical transmission measurements at various wavelengths using the relationship given by Sunds [14, 15].

$$\alpha = -\frac{1}{t} \ln(T) \quad (1)$$

where  $T$  is transmittance and  $t$  is film thickness.

The  $t$  of the thin film can be determined from the interference fringes of transmission data by calculating the refractive index of the thin film corresponding to two adjacent maxima (or minima) given as  $n(\lambda_1)$  at  $\lambda_1$  and  $n(\lambda_2)$  at  $\lambda_2$  [16],

$$t = \frac{\lambda_1 \lambda_2}{2(n(\lambda_2)\lambda_1 - n(\lambda_1)\lambda_2)} \quad (2)$$

where  $n(\lambda_1)$  and  $n(\lambda_2)$  are the refractive indices in two consecutive maxima (or minima) and  $\lambda_1$  and  $\lambda_2$  the corresponding wavelengths. The thickness of annealed films estimated from transmission measurements and surface stylus profilometer are listed in Table 3.

The band gap values were estimated considering the CoFe<sub>2</sub>O<sub>4</sub> as a direct band gap material, by using the well-known Tauc's formula [16, 17],

$$\alpha h\nu = A(h\nu - E_g)^{1/2}$$

**Table 3** Optical properties of CoFe<sub>2</sub>O<sub>4</sub> thin films deposited at various RF powers

Sample	Film thickness ( $\pm 5$ nm)		Band gap, $E_g$ ( $\pm 0.02$ eV)		
	As-grown	Annealed	As-grown	Annealed	
	Profiler	Profiler	Calculated		
CFF-60	124	119	–	2.16	2.30
CFF-80	180	164	147	2.11	2.16
CFF-100	269	237	258	2.14	2.20
CFF-120	300	286	294	2.08	2.25

where  $A$  is constant,  $\alpha$  is the optical absorption coefficient, and  $h\nu$  is the energy of the incident photon. Figure 10 shows the plots of  $(\alpha h\nu)^2$  versus  $h\nu$  for the annealed CoFe<sub>2</sub>O<sub>4</sub> thin films. The extrapolation of the straight-line graphs to  $(\alpha h\nu)^2 = 0$  gives the value of the optical gap. It can be seen that the plots of  $(\alpha h\nu)^2$  versus  $(h\nu)$  varies linearly for all the films in the region of strong absorption near the fundamental absorption edge over a wide range of photon energies.

The linear variation of absorption coefficient at high frequencies indicates that these thin films have direct transitions across the energy band gap. The estimated values of energy band gap for the as-deposited and annealed films are listed in Table 3. The error in the optical band gap measurement by linear curve fitting is  $\pm 0.02$  eV. The band gap variation for films deposited at 80–120 W of RF power is within this measurement error limits. The increase in the optical band gap of CoFe<sub>2</sub>O<sub>4</sub> thin films by annealing may be due to the removal of defect levels from the films. The optical band gap for annealed films shows a decrease from 2.3 to 2.16 eV as the RF power increases from 60 to 80 W and shows variations within the experimental

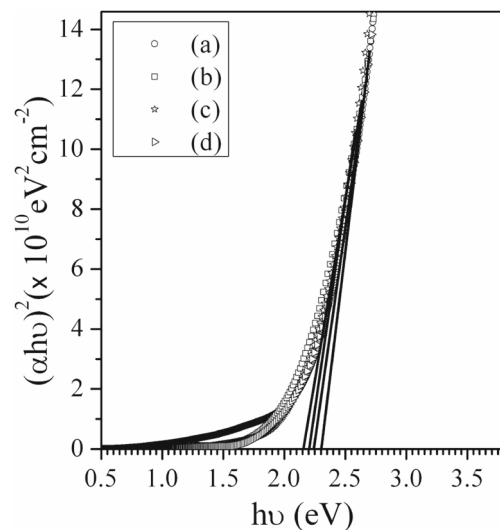


**Fig. 10** Plots of  $(\alpha h\nu)^2$  versus  $(h\nu)$  for annealed CoFe<sub>2</sub>O<sub>4</sub> thin films deposited at **a** 60, **b** 80, **c** 100, and **d** 120 W RF powers



error thereafter. This could be attributed to smaller average grain size in the thinner film (119 nm) deposited at 60 W, compared with that in the thicker film (164 nm) deposited at 80 W. The estimated  $E_g$  value for the annealed  $\text{CoFe}_2\text{O}_4$  thin film deposited at 60 W (120 nm) is 2.3 eV, which is smaller than 2.6 eV reported by Erdem et al. [18] for a 100-nm-thick  $\text{CoFe}_2\text{O}_4$  thin film deposited by spin coating. The estimated direct band gap values for annealed films are greater than those reported by Rao et al. [19] and smaller than those reported by Ravindra et al. [8] and Holinsworth et al. [20].

## 4 Conclusions

Cobalt-ferrite thin films were deposited on glass substrates by radio-frequency magnetron sputtering using ceramic  $\text{CoFe}_2\text{O}_4$  target in Ar gas environment. The grazing incidence X-ray diffraction studies reveal the nanocrystalline nature of the films. The average grain size and particle size or crystallite size of the film is found to increase first and then decrease with increase in RF power. The films are highly transparent above 600 nm wavelength. The saturation magnetization, remanence, and coercivity first decrease as the RF power increases from 60 to 80 W and then increase with further increase in the RF power. The optical band gap decreases on annealing the films. The optical band gap first decreases as the RF power increases from 60 at 80 W followed by an increasing trend with a further increase in RF power. The observed changes in the properties of the film are due to the combined effect of grain size and cation distribution.

## References

- Fontijn, W.F.J., van der Zaag, P.J., Feiner, L.F., Metselaar, R., Devillers, M.A.C.: A consistent interpretation of the magneto-optical spectra of spinel type ferrites (invited). *J. Appl. Phys.* **85**, 5100 (1999)
- Suzuki, A.Y.: Epitaxial spinel ferrite thin films. *Ann. Rev. Mater. Res.* **31**, 265 (2001)
- Ramos, A.V., Santos, T.S., Miao, G.X., Guittet, M.-J., Moussy, J.-B., Moodera, J.S.: Influence of oxidation on the spin-filtering properties of  $\text{CoFe}_2\text{O}_4$  and the resultant spin polarization. *Phys. Rev. B* **78**, 180402 (R) (2008)
- Bouet, L., Tailhades, P., Rousset, A.: Relations between magneto-optical properties and reactivity in cobalt-manganese ferrite thin films and powders. *J. Magn. Magn. Mater.* **153**, 389 (1996)
- Rondinone, A.J., Samia, A.C., Zhang, Z.J.: Characterizing the magnetic anisotropy constant of spinel cobalt ferrite nanoparticles. *Appl. Phys. Lett.* **76**, 3624 (2000)
- Sultan, M., Singh, R.: Magnetic and optical properties of RF-sputtered zinc ferrite thin films. *J. Appl. Phys.* **105**, 07A512 (2009)
- Chavan, S.M., Babrekar, M.K., More, S.S., Jadhav, K.M.: Structural and optical properties of nanocrystalline Ni–Zn ferrite thin films. *J. Alloy Comput.* **507**, 21 (2010)
- Ravindra, A.V., Padhan, P., Prellier, W.: Electronic structure and optical band gap of  $\text{CoFe}_2\text{O}_4$  thin films. *Appl. Phys. Lett.* **101**, 161902 (2012)
- Sultan, M., Singh, R.: Structural and optical properties of RF-sputtered  $\text{ZnFe}_2\text{O}_4$  thin films. *J. Phys. D* **42**, 115306 (2009)
- Zhang, Y., Du, G., Liu, D., Wang, X., Ma, Y., Wang, J., Yin, J., Yang, X., Hou, X., Yang, S.: Crystal growth of undoped ZnO films on Si substrates under different sputtering conditions. *J. Cryst. Growth* **243**, 439 (2002)
- Patterson, A.L.: The Scherrer formula for X-ray particle size determination. *Phys. Rev.* **56**, 978 (1939)
- Lee, J.-G., Chae, K.P., Sur, J.C.: Surface morphology and magnetic properties of  $\text{CoFe}_2\text{O}_4$  thin films grown by a RF magnetron sputtering method. *J. Magn. Magn. Mater.* **267**, 161 (2003)
- Wang, Y.C., Ding, J., Yi, J.B., Liu, B.H., Yu, T., Shen, Z.X.: High-coercivity Co-ferrite thin films on (100)- $\text{SiO}_2$  substrate. *Appl. Phys. Lett.* **84**, 14 (2004)
- Sunds, R.H.: Paramagnetic resonance absorption in glass. *Phys. Rev.* **99**, 1222 (1955)
- Davis, E.A., Mott, N.F.: Conduction in non-crystalline systems. V. Conductivity, optical absorption and photoconductivity in amorphous semiconductor. *Philos. Mag.* **22**, 903 (1970)
- Tauc, J., Grigorovici, R., Vancu, A.: Optical properties and electronic structure of amorphous germanium. *Phys. Status Solidi* **15**, 627 (1966)
- Tauc, J.: *Amorphous and Liquid Semiconductors*. Plenum, New York (1974)
- Erdem, D., Bingham, N.S., Heiligt, F.J., Pilet, N., Warnicke, P., Heyderman, L.J., Niederberger, M.:  $\text{CoFe}_2\text{O}_4$  and  $\text{CoFe}_2\text{O}_4$ - $\text{SiO}_2$  nanoparticle thin films with perpendicular magnetic anisotropy for magnetic and magneto-optical applications. *Adv. Func. Mater.* **26**, 1954 (2016)
- Rao, P., Godbole, R.V., Phase, D.M., Chikate, R.C., Bhagwat, S.: Ferrite thin films: synthesis, characterization and gas sensing properties towards LPG. *Mater. Chem. Phys.* **149–150**, 333 (2015)
- Holinsworth, B.S., Mazumdar, D., Sims, H., Sun, Q.-C., Yurtisigi, M.K., Sarker, S.K., Gupta, A., Butler, W.H., Musfeldt, J.L.: Chemical tuning of the optical band gap in spinel ferrites:  $\text{CoFe}_2\text{O}_4$  vs  $\text{NiFe}_2\text{O}_4$ . *Appl. Phys. Lett.* **103**, 082406 (2013)